Neurotoxicity Research (2019) 36:736–745
https://doi.org/10.1007/s12640-019-00075-1

ORIGINAL ARTICLE

Distinct Impacts of Fullerene on Cognitive Functions of Dementia vs. Non-dementia Mice

Yawen Wu[1] · Runzi Wang[1] · Yuexiang Wang[1] · Jing Gao[1] · Lina Feng[1] · Zhuo Yang[1]

Received: 30 March 2019 / Revised: 1 June 2019 / Accepted: 11 June 2019 / Published online: 20 June 2019

Abstract

Fullerene is a family of carbon materials widely applied in modern medicine and ecosystem de-contamination. Its wide application makes human bodies more and more constantly exposed to fullerene particles. Since fullerene particles are able to cross the blood-brain barrier (BBB) (Yamago et al. 1995), if and how fullerene would affect brain functions need to be investigated for human health consideration. For this purpose, we administered fullerene on subcortical ischemic vascular dementia (SIVD) model mice and sham mice, two types of mice with distinct penetration properties of BBB and hence possibly distinct vulnerabilities to fullerene. We studied the spatial learning and memory abilities of mice with Morris water maze (MWM) and the neuroplasticity properties of the hippocampus. Results showed that fullerene administration suppressed outcomes of MWM in sham mice, along with suppressed long-term potentiation (LTP) and dendritic spine densities. Oppositely, recoveries of MWM outcomes and neuroplasticity properties were observed in fullerene-treated SIVD mice. To further clarify the mechanism of the impact of fullerene on neuroplasticity, we measured the levels of postsynaptic density protein 95 (PSD-95), synaptophysin (SYP), brain-derived neurotrophic factor (BDNF), and tropomyosin receptor kinase B (TrkB) by western blot assay. Results suggest that the distinct impacts of fullerene on behavior test and neuroplasticity may be conducted through postsynaptic regulations that were mediated by BDNF.

Keywords Fullerene · Subcortical ischemic vascular dementia (SIVD) · Long-term potentiation (LTP) · Hippocampus · Neuroplasticity

Introduction

Fullerene is a family of carbon materials in the form of hollow spheres consisting of C_{60} or C_{70} and was firstly discovered by H. Kroto, R. Smalley, and R. Curl in 1985 (Kroto et al. 1985) who were awarded the Nobel Prize in chemistry in 1996 for their discovery. Due to the excellent absorption and antimicrobial properties (Lyon et al. 2010) as well as its relatively low cost, fullerene has been widely applied in modern water treatment and ecosystem de-contamination (Chae et al. 2014; Narita et al. 2004). In modern medical applications, fullerene and its derivatives have been suggested as promising therapeutic agents as well as a good candidate for drug delivery (Prylutskyy et al. 2017; Zhou 2013). Water-soluble fullerene has been reported to be able to absorb free radicals, promote skeletal muscle regeneration (Ishii et al. 2013; Ishii et al. 2014), and inhibit arthritis (Yudoh et al. 2009b; Yudoh et al. 2009a). Podolski and co-workers conducted extensive studies on the anti-amyloid effect of fullerene and its potentials in treating Alzheimer's disease, in the aspects of reversing cognition impairment, preventing neurodegeneration and protecting neuroplasticity (Gordon et al. 2017; Makarova et al. 2012; Podlubnaya et al. 2006; Podolski et al. 2010; Podolski et al. 2007; Vorobyov et al. 2015).

However, in other scientific studies, cytotoxicity of fullerene was reported in several cell lines (Irie et al. 1996; Yamawaki and Iwai 2006) as well as in vivo on rodents and other animal species (Sayes et al. 2007; Usenko et al. 2007; Yamago et al. 1995). Since fullerene particles are able to cross the blood-brain barrier (BBB), the brain becomes an accessible organ of fullerene circulation in body (Yamago et al. 1995)

Yawen Wu, Runzi Wang and Yuexiang Wang contributed equally to this work.

✉ Zhuo Yang
zhuoyang@nankai.edu.cn

[1] College of Medicine, State Key Laboratory of Medicinal Chemical Biology, Key Laboratory of Bioactive Materials for Ministry of Education, Nankai University, Tianjin 300071, China

and pathological conditions involving BBB leakage may be more vulnerable or sensitive to the presence of fullerene as compared with intact brains. These studies suggest that whether the impact of fullerene is beneficial or toxic needs to be evaluated according to the physiological/pathological conditions of the subject. Under the pathological conditions of dementia caused by vascular ischemia, fullerene may play a quite different role compared with that in normal brain due to the high oxidative stress of ischemic brain environment (Friberg et al. 2002; Love 1999; Murín et al. 2001; Radak et al. 2013), and the outstanding absorption properties and the free radical scavenger effect of fullerene may be beneficial in this context. Hence, we hypothesize that fullerene particles would impact brain functions of dementia and non-dementia mice differently due to the different brain environments.

To test this hypothesis, we established subcortical ischemic vascular dementia (SIVD) model on mice and approached the effect of fullerene administration on the learning and memory abilities of SIVD mice by Morris water maze (MWM) test and the underlying neuroplasticity of mouse hippocampus, an important brain region deeply involved in learning and memory (Squire 2004), and we compared that with the fullerene effect on sham/non-dementia mice. To study the underlying neuroplasticity, long-term potentiation (LTP) and dendritic spine densities, important electrophysiological and structural features of neuroplasticity were monitored. We further quantified the levels of postsynaptic density protein 95 (PSD-95), synaptophysin (SYP), brain-derived neurotrophic factor (BDNF), and tropomyosin receptor kinase B (TrkB), important proteins responsible for neuroplasticity regulation by western blot assay. We found that chronic fullerene treatment (50 mg/kg, i.p., two weeks) substantially improved the learning and memory abilities and related neuroplasticity properties in SIVD mice but undermined these abilities/properties of sham mice. Further, our western blot results suggested that PSD-95, a family member of membrane-associated guanylate kinase that exclusively located on postsynaptic density of neurons (Hunt et al. 1996) and BDNF, an important protein that mediated neuroplasticity (Cunha et al. 2010; Gottmann et al. 2009; Leßmann and Brigadski 2009; Lu 2003), played important roles in the effects of fullerene on neuroplasticity. Our findings of the different impacts of fullerene on subjects with different physiological/pathological conditions provided novel and useful insights in future application of fullerene.

Materials and Methods

Materials and Chemicals

Fullerene (C_{60}) used in this study was purchased from Ailan Chemical Technology Co. Ltd. (Shanghai, China) without modification. The fullerene powder was suspended in 0.9% NaCl with 0.1% Tween 80 then sonicated for 20 min before use. Golgi-Cox staining kits were purchased from Keyijiaxin, Tianjin, China. Chemicals for western blot assay were purchased from Beyotime Biotechnology (Haimen, China). All the solutions were prepared in distilled water.

Primary antibodies of anti-β-actin (1:5000), anti-SYP antibody (1:2000), anti-PSD 95 antibody (1:2000), anti-TrkB antibody (1:2000), anti-BDNF antibody (1:2000) were purchased from Abcam (Cambridge, UK). The anti-mouse (1:5000) secondary antibodies were obtained from Promega (Promega Co., USA).

Fullerene Characterization

The suspension of fullerene particles was characterized by a transmission electron microscope (JEM-2800, JEOL Ltd., Tokyo, Japan) as shown in Fig. 1. Zeta potential was measured with a Zeta-PALS+BI-90 Plus (Brookhaven Instruments Corp., USA) at a fixed wavelength of 659 nm and a scattering angle of 90°.

Animals and Surgery

Adult specific-pathogen-free (SPF) male C57BL/6L mice (eight weeks old), weighing 18–22 g, were purchased from the Experimental Animal Center of Chinese Academy of Medical Science. Mice were housed at 12:12 h light/dark cycle with food and water ad libitum. All experiments were performed according to protocols approved by the

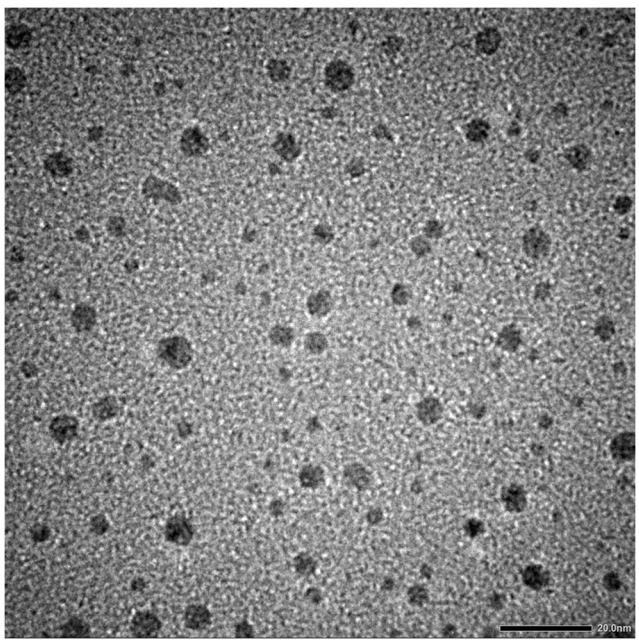

Fig. 1 TEM image of fullerene particles (dark spots) in suspension. Scale bar 20 nm

Committee for Animal Care of Nankai University and in accordance with the practices outlined in the NIH Guide for the Care and Use of Laboratory Animals.

All the mice were randomly divided into four groups (five mice in each group): sham, sham-fullerene (sham-F), SIVD, and SIVD-fullerene (SIVD-F). All the mice received either SIVD or sham surgery that was performed as follows. After overnight fasting, mice were anesthetized by sodium pentobarbital (45 mg/kg, i.p.). After checking their anesthesia with forceps, neck skin was cut open to expose the right common carotid artery of the mouse. Then the nerves and surrounding tissues were cleared away from the artery. For SIVD and SIVD-F groups, mouse right carotid artery was permanently occluded with suture. As for sham and sham-F groups, the suture was loosely knotted around the carotid artery. After wound suturing, antibiotic was given by intramuscular injection, and mice were placed on heating blankets to keep warm until awake. All the mice were allowed 3 days for recovery before fullerene or saline administration.

For the groups of sham-F and SIVD-F, the mice received an intraperitoneal injection of 50 mg/kg fullerene (suspended in a solution containing 0.9% NaCl and 0.1% Tween 80) once each day for two weeks. For the groups of sham and SIVD, mice received intraperitoneal injections of blank saline solution (containing 0.9% NaCl and 0.1% Tween 80) once each day for two weeks.

Morris Water Maze

After the 2-week treatment with fullerene or blank saline, all the mice were subjected to the Morris water maze test (MWM, RB-100A type, Beijing, China) to assess the spatial learning and memory abilities. The MWM system contained a 90-cm-diameter maze filled with water. The water inside the maze was stained white with non-toxic TiO_2 and the water temperature was kept at 25 ± 1 °C. The swimming activity of mice was captured by a video camera and analyzed by a personal computer. On the computer software, the swimming arena was equally divided into 4 quadrants (I–IV) and a 9-cm-diameter platform was placed in the center of quadrant I and submerged 0.5–1 cm below the water surface during the initial training stage.

During the initial training stage, all the mice were trained for four days with four trials each day. In each trial, the mouse was gently put onto the water surface at a random point of each quadrant. The time spent to find the hidden platform (escape latency) and the swimming speed of each mouse were recorded. If the mouse failed to find the platform within 60 s, the experimenter would guide the mouse and let the mouse stay on the platform for 10 s, and the escape latency of this mouse would be recorded as 60 s. The time interval between trials was no less than 10 min to make sure all the mice got sufficient rest. After the training stage, all the mice were subjected to spatial probe test 24 h after the last training trial. During the test, the platform was removed and the mouse was gently put onto the water at the opposite quadrant (IV). The mouse was allowed to swim freely for 60 s, and the target quadrant dwell time (time spent in quadrant I) and platform crossings were recorded on the computer.

In vivo Electrophysiological Study

LTP recording protocols were similar to those described in our previous study (An et al. 2012; Gao et al. 2015; Han et al. 2013). Briefly, after being anesthetized with 30% (*w*/*w*) urethane (0.4 mL/kg, i.p.), the mice were positioned on a stereotaxic frame (SR-6 N; Narishige, Japan). After exposure of the skull, holes were drilled at proper sites for the location of a recording electrode and a bipolar stimulating electrode. The stimulating electrode was implanted in the perforant pathway (PP: − 3.8 mm AP, 3.0 mm ML, 1.5 mm DV) and the recording electrode was positioned in dentate gyrus region of the hippocampus (DG: − 2.0 mm AP, 1.4 mm ML, 1.5 mm DV) (Paxinos and Franklin 2007). Electrode positions were optimized by slowly dialing down the electrodes while recording the single stimulation pulse (0.2-ms duration, 0.3 mA) evoked responses. Then the stimulation intensity was tuned from 0.1 to 1 mA with 0.1 mA increment. The stimulation intensity evoking a response of 50–60% of the maximal was chosen for the following experiments. After the stimulation intensity optimization, 30 single pulse evoked responses were recorded every 1 min as a baseline. Then a theta burst stimulation (TBS, 30 trains of 6 pulses at 100 Hz) was delivered through a stimulating electrode to induce LTP. Then 60 single pulse evoked responses were recorded after TBS. All the raw data were analyzed in Clampfit 10.0 (Molecular Devices, Sunnyvale, CA). After the electrophysiological experiment, the mice were sacrificed and the brains were removed for Golgi-Cox staining or western blot assay.

Golgi-Cox Staining

The protocols of Golgi-Cox staining were similar to those described in previous literatures (Narayanan et al. 2014) with modifications. Briefly, the bulk solution for Golgi-Cox staining was prepared with the following solutions from the commercial kit: (A) 200 mL of 5% $K_2Cr_2O_7$; (B) 200 mL of 5% $HgCl_2$; (C) 560 mL of 5% K_2CrO_4. Firstly, solutions A and B were mixed slowly and thoroughly. Then the mixture was added into solution C and mixed thoroughly. After staying in dark for 3 h, the final mixture solution was filtered and stored in dark until use.

The mice were sacrificed after electrophysiological experiments under anesthesia of 30% (*w*/*w*) urethane (0.4 mL/kg, i.p.). After sacrifice, the whole mouse brain for Golgi-Cox staining was dissected out carefully and the cerebella were

removed. The hemisphere with hippocampus inside was kept in the filtered solution for Golgi-Cox staining for two weeks. Each stained hemisphere was cut into coronal slices with a thickness of 150 μm on a vibrating blade microtome (Leica VT1000S, Leica Biosystems, Nussloch, Germany). Then the brain slices containing hippocampus inside were selected to be immersed into 6% Na_2CO_3 for 20 min then transferred into a series of EtOH solutions for dehydration: 70% EtOH (10 min), 90% EtOH (15 min), and 100% EtOH (20 min). Then the dehydrated brain slices were immersed into xylene for 20 min for transparency. Then the brain slices were sealed on glass slides with neutral balsam (Solarbio, Beijing, China) and covered with a coverslip.

Dendritic Spine Imaging and Analysis

A Leica upright fluorescence microscope system (Leica DM3000 (lens), Leica Biosystems, Nussloch, Germany) integrated with a digital camera (Leica DFC420 (CCD)) was used for imaging Golgi-Cox stained brain slices. The dendritic spine densities of neurons in the DG region of the mouse hippocampus (the same location of electrophysiological recordings: − 2.0 mm AP, 1.4 mm ML, 1.5 mm DV, but of the other brain hemisphere) were analyzed and quantified with ImageJ and NeuronStudio software (Dumitriu et al. 2011; Narayanan et al. 2014; Rodriguez et al. 2008). Fifteen dendrites with a length of no less than 10 μm were quantified in each animal for averaging (Dumitriu et al. 2011).

Western Blot Assay

After sacrifice, the mouse hippocampi were dissected out and kept frozen at − 80 °C. Before western blot assay, the hippocampi were lysed in a 200-μL protein lysis buffer (RIPA buffer contents: 50 mM Tris (pH 7.4), 150 mM NaCl, 1% NP-40, 0.5% sodium deoxycholate; Solarbio Science & Technology Co., Ltd., Beijing, China) containing phenylmethanesulfonyl fluoride (PMSF 1:100; Beyotime Biotechnology, Haimen, China). The lysate was centrifuged at 12,000*g* for 20 min at 4 °C. Then the supernatant was mixed thoroughly with a loading buffer (4:1). The mixture was then boiled for 20 min and followed by electrophoresis in 10–13% SDS-PAGE gel. Then the separated protein bands were transferred onto the polyvinylidene fluoride (PVDF) membranes (0.45 μm) and then incubated with 5% skim milk followed by primary antibody incubation overnight at 4 °C. The next day, after being washed three times with TBST, the protein bands on PVDF membranes were incubated with secondary antibody. The protein bands were visualized on a chemiluminescence detection kit (Pierce) and exposed to an X-ray film (Eastman Kodak, Rochester, NY). Internal control was ensured by using β-actin expression using a mouse monoclonal antibody (1:1000; Santa Cruz).

Statistics

All the figures were plotted with OriginPro 8. The data in Fig. 2 a and b were analyzed with two-way ANOVA with

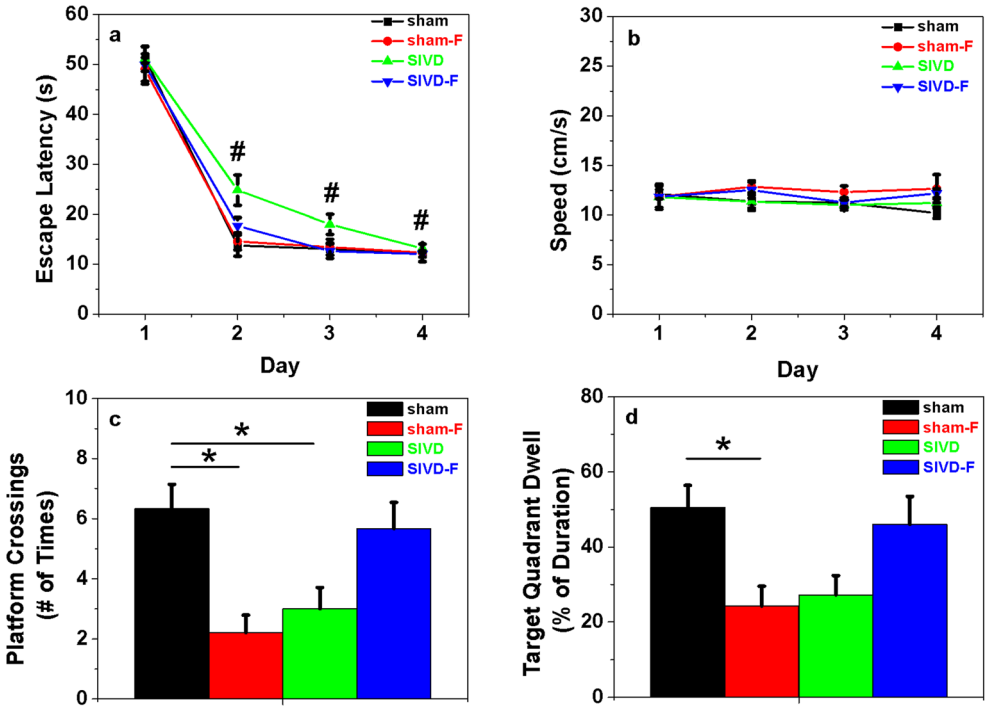

Fig. 2 Morris water maze results. **a** Escape latencies during training days. **b** Swimming speeds during training days. **c** Platform crossings the on test day. **d** Target quadrant dwell time shown as the percentage of time spent in this quadrant on the test day. Data were presented as mean ± SEM. $^{*}p < 0.05$, $^{\#}p < 10^{-10}$

repeated measurements. Data in all the other figures were subjected to one-way ANOVA. Post hoc comparison was performed with the Tukey test, and $p < 0.05$ was considered significantly different.

Results

Characterization of Fullerene Particles

The morphology of fullerene particles in suspension was characterized by TEM, as demonstrated in Fig. 1. The particle size was 4.22 ± 0.15 nm. The zeta potential of fullerene particles in suspension was − 39.34 mV.

Mouse Body Weight During Fullerene Administration

At the end of the 2-week administration of either fullerene or blank saline, mouse body weights were slightly lower in SIVD (23.4 ± 0.4 g) and SIVD-F (24.1 ± 0.8 g) groups than those of sham (24.9 ± 0.7 g) and sham-F (25.1 ± 0.7 g) groups, probably due to the ligation. Fullerene administration did not cause body weight loss either in sham or SIVD mice. Actually, the body weights of mice receiving fullerene injections were slightly higher than those of mice receiving blank saline injections. But when subjected to statistical analysis of the one-way ANOVA, the group factor of the last day body weight was not significant ($n = 5$, $F(3,16) = 1.40$, $p = 0.3$). These results suggested that at the end of the 2-week administration of fullerene or blank saline, neither our surgery nor fullerene administration caused damage to the whole healthiness of mice.

Effects of Fullerene on MWM Outcomes of Sham vs. SIVD Mice

As shown in Fig. 2a, all the four groups of mice spent less time to find the platform in the following days of training stage suggesting efficient learning of all the groups. Data in Fig. 2a were subjected to the two-way ANOVA with repeated measurements (days). Both group factor ($n = 5$, $F(3,16) = 8.45$, $p = 0.0014$) and day factor ($n = 5$, $F(3,48) = 319.2$, $p = 1.1 \times 10^{-31}$) were significant. On day two, the escape latency of group SIVD was significantly higher as compared with sham (sham vs. SIVD, $p < 0.05$), and the escape latency of group SIVD-F was significantly lower than that of SIVD (SIVD vs. SIVD-F, $p < 0.05$) according to post hoc comparison. This suggests a deficit of learning and memory abilities in the SIVD group, probably because dementia and fullerene administration could partially rescue this deficit. In the following training days (3rd and 4th), the difference disappeared and all the groups demonstrated similar escape latencies towards the end of the training. Figure 2 b showed the swimming speed of all the groups of mice during the training stage. Neither the group factor ($n = 5$, $F(3,16) = 2.10$, $p = 0.14$) nor the day factor ($n = 5$, $F(3,48) = 0.43$, $p = 0.73$) was significant showing similar swimming abilities of all the groups of mice.

On the test day, the learning and memory abilities of mice were presented as platform crossings and target quadrant dwell percentage, as shown in Fig. 2 c and d. In the platform crossings results, the group factor was significant ($n = 5$, $F(3,16) = 6.66$, $p = 0.003$). Fullerene administration decreased the platform crossings significantly in sham mice (sham vs. sham-F, $p < 0.05$). However, in SIVD mice, the effect of fullerene was quite different. When comparing with the sham group, platform crossings were significantly suppressed in the SIVD group (sham vs. SIVD, $p < 0.05$), and fullerene administration improved the platform crossings to the level similar to that of the sham group (sham vs. SIVD-F, $p > 0.05$). The target quadrant dwell percentage results demonstrated similar trends. The group factor of the target quadrant dwell percentage was significant ($n = 5$, $F(3,16) = 4.58$, $p = 0.015$) and the difference between sham and sham-F was significant ($p < 0.05$), though the difference between SIVD and sham did not reach a significant level. These results suggested that fullerene exhibited distinct impacts on mice with different penetration properties of BBB (sham vs. SIVD): fullerene impaired the memory formation of sham mice, but in mice with SIVD, fullerene was beneficial.

Effects of Fullerene on LTP Results of Sham vs. SIVD Mice

Figure 3 a showed the normalized slopes of field excitatory postsynaptic potential (fEPSP) responses before and after TBS, and fEPSPs slopes were normalized against the slopes of the baseline of each individual mouse. In the sham group, TBS induced a substantial increase of fEPSPs slopes and fullerene administration suppressed fEPSPs slope elevation dramatically in the sham-F group. However, in SIVD mice, fullerene improved LTP responses of the SIVD-F group substantially as compared with that of the SIVD group. We further quantified the normalized fEPSPs slopes of the last 10 min of LTP recordings in Fig. 3b and the group factor was significant ($n = 5$, $F(3,16) = 4.88$, $p = 0.014$). In sham mice, fullerene administration suppressed fEPSPs slopes to a significant level (sham vs. sham-F, $p < 0.05$), which suggests a harmful impact of fullerene on LTP of sham mice. However, for SIVD mice, the average of the last 10 min fEPSPs slopes was substantially suppressed as compared with that of the sham group (sham vs. SIVD, $p < 0.05$) showing the neuroplasticity deficits caused by SIVD, but fullerene administration partially reversed this suppression and tended to elevate fEPSPs slopes to the level similar to that of sham group (sham vs. SIVD-F, $p > 0.05$). These results suggest a beneficial effect of fullerene

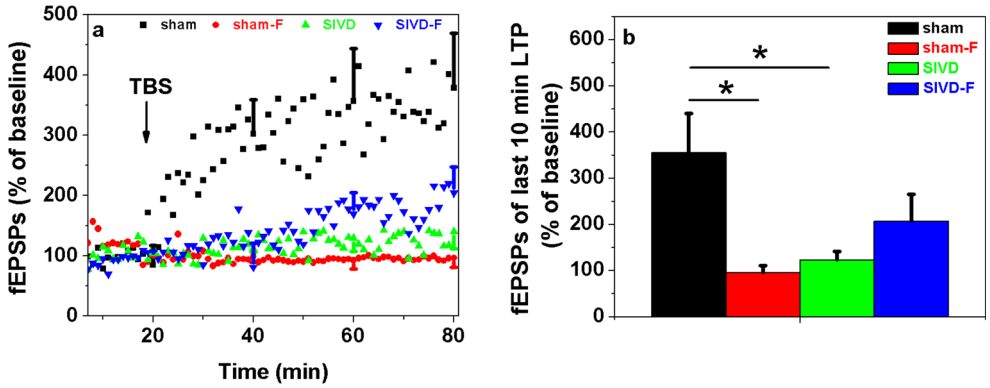

Fig. 3 Normalized slopes of fEPSPs in response to TBS. **a** Normalized slopes of fEPSPs before and after TBS (arrow pointed at stimulation time). **b** Mean values of normalized slopes of the last 10 min of LTP recordings. Slopes of fEPSPs were normalized against the baseline of each mouse. Data were presented as mean ± SEM. *$p < 0.05$

administration on LTP results of SIVD mice, but a harmful effect on sham mice that is in line with our MWM results.

Dendritic Spine Densities in DG of Mouse Hippocampus

Dendritic spine densities are well known to be the structural basis of neuroplasticity. To further investigate the impact of fullerene particles on neuroplasticity in sham vs. SIVD mice, we quantified the dendritic spine densities in the DG region of mouse hippocampus (Fig. 4). Our results showed that the group factor of dendritic spine densities was significant ($n = 5$, $F(3,16) = 4.79$, $p = 0.015$) as analyzed by the one-way ANOVA. Fullerene administration significantly suppressed the dendritic spine density in sham mice (Fig. 4d; sham vs. sham-F, $p < 0.05$) suggesting a harmful effect of fullerene on sham mice. On the other hand, fullerene administration rescued the suppression of dendritic spine density of SIVD mice (Fig. 4d; sham vs. SIVD, $p < 0.05$) by elevating the spine density to the level not significantly different from sham

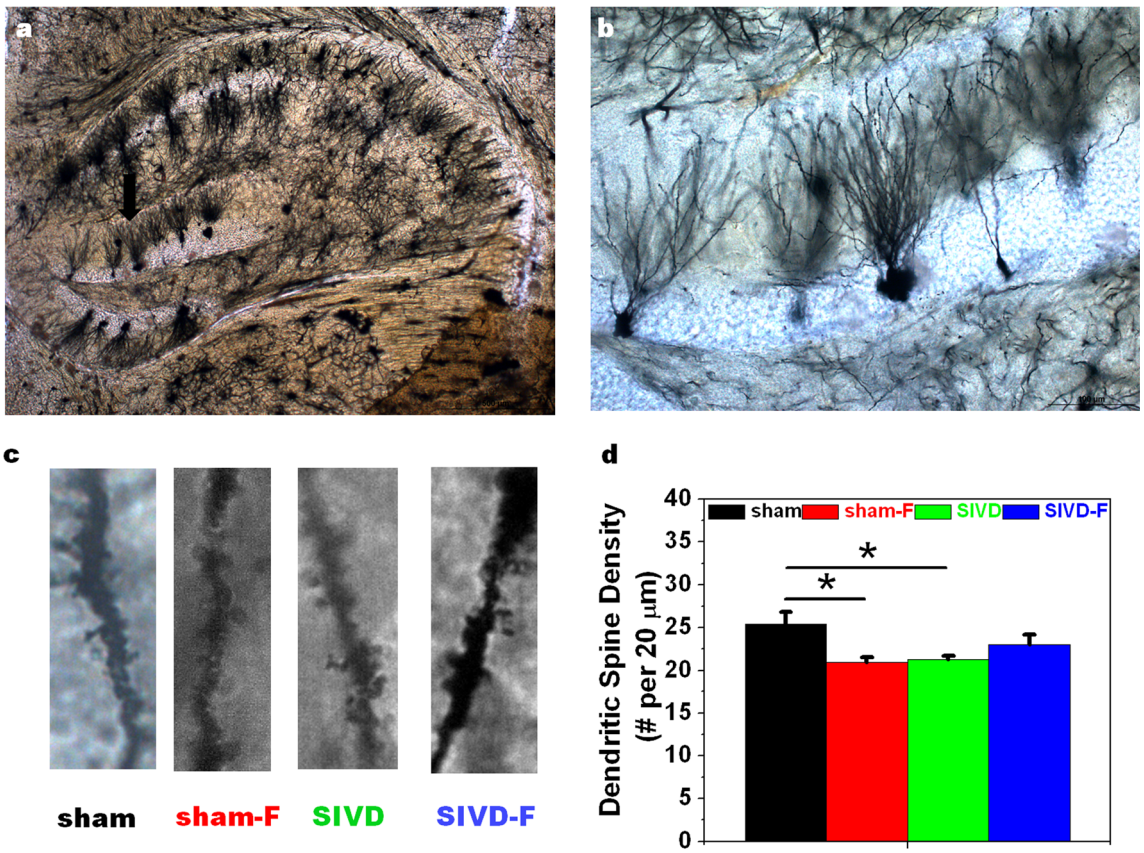

Fig. 4 Dendritic spines in the DG region of mouse hippocampus. **a** Golgi-Cox stained mouse hippocampus (black arrow pointed at DG). **b** Neurons in DG. **c** Dendrite examples of each group. **d** Dendritic spine densities in each group. Data were presented as mean ± SEM. *$p < 0.05$

(sham vs. SIVD-F, $p > 0.05$). These results supported our MWM and LTP observations showing that fullerene had a beneficial effect on the neuroplasticity of SIVD mice but being harmful to sham, on the structural level.

Neuroplasticity Related Protein Levels

To investigate the underlying mechanisms of the beneficial effect of fullerene on the neuroplasticity of SIVD mice, we quantified important proteins that were responsible or could mediate neuroplasticity by western blot assay. As demonstrated in Fig. 5b, the group factor of PSD-95 contents was significant ($n = 3$, $F(3,8) = 11.9$, $p = 0.003$) according to the one-way ANOVA. PSD-95 in sham-F was significantly lower than that in the sham group (sham vs. sham-F, $p < 0.05$). PSD-95 in the SIVD group was significantly lower than that in the sham group (sham vs. SIVD, $p < 0.05$) and fullerene administration significantly increased the level of PSD-95 in SIVD mice (SIVD vs. SIVD-F, $p < 0.05$) to the level similar to that in the sham group (sham vs. SIVD-F, $p > 0.05$). These results suggest that the harmful effect of fullerene on sham mice and at the same time the beneficial effect of fullerene on SIVD mice may be conducted through postsynaptic regulations.

To investigate the presynaptic regulations, we quantified the contents of SYP, an important protein located on the presynaptic terminals. As analyzed by the one-way ANOVA, the group factor was not significant ($n = 3$, $F(3,8) = 0.37$, $p = 0.8$). These results suggest a non-significant effect of fullerene or SIVD surgery on SYP levels, and presynaptic regulations may play a minor role in these cases.

We quantified the contents of BDNF in mouse hippocampus as demonstrated in Fig. 5d. The one-way ANOVA demonstrated that the group factor was significant ($n = 3$, $F(3,8) = 6.1$, $p = 0.02$). BDNF levels of sham-F and SIVD were suppressed as compared with those of the sham group, but not to significant levels (sham vs. sham-F, $p > 0.05$; sham vs. SIVD, $p > 0.05$). On the other hand, fullerene administration significantly increased BDNF content in SIVD-F mouse hippocampus (SIVD vs. SIVD-F, $p < 0.05$), suggesting a beneficial effect of fullerene on BDNF of dementia subjects.

BDNF can be released into extracellular space and change the excitatory state of neurons through binding to its receptor TrkB. Our results demonstrated that the group factor of TrkB contents was not significant ($n = 3$, $F(3,8) = 0.16$, $p = 0.9$). These results suggest that the extracellular BDNF may play a more predominant role in mediating neuroplasticity in these cases.

Discussion

For non-pathological subjects, fullerene exposure was reported to cause oxidative stress in embryonic zebrafish (Usenko et al. 2008) and juvenile largemouth bass brain (Oberdörster 2004), probably due to lipid peroxidation (Sayes et al. 2005). However, in the biological systems under high oxidative stress, the structures of fullerene and its derivatives rendered them as potential scavengers for reactive oxygen species (Geckeler and Samal 2001; Yin and Xu 2002; Yin et al. 2009). Extensive research works by Dugan and co-workers demonstrated the free radical scavenger and anti-oxidative effect of fullerene, and its derivatives can attenuate cytotoxicity of the nervous system (Ali et al. 2008; Ali et al. 2004; Dugan et al. 1996; Dugan et al. 1997; Quick et al. 2008). And the neuroprotection effect was confirmed in neurodegenerative disease models such as Parkinson's disease (Dugan et al. 2001; Dugan et al. 2014) and Alzheimer's disease

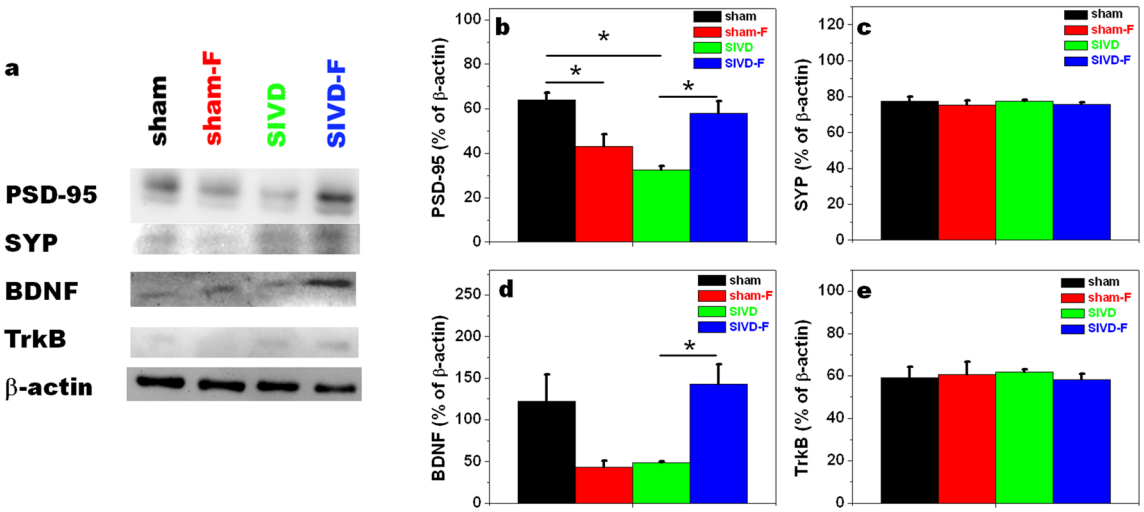

Fig. 5 Contents of neuroplasticity related proteins. **a** Examples of protein bands. **b**–**e** Relative levels of protein (PSD-95, SYP, BDNF, and TrkB, respectively) in mouse hippocampus. Data were presented as mean ± SEM. *$p < 0.05$

(Gordon et al. 2017; Makarova et al. 2012; Podlubnaya et al. 2006; Podolski et al. 2010; Podolski et al. 2007; Vorobyov et al. 2015). Podolski and co-workers demonstrated that the anti-amyloid effect of hydrated fullerene could reverse the impairment of cognitive performance of rats induced by $A\beta_{25–35}$ injection (Gordon et al. 2017; Podolski et al. 2007), probably through inhibiting the fibrillization of $A\beta_{25–35}$ peptide (Podolski et al. 2007). An in vitro study suggested an aqueous molecule-colloidal solution of C_{60} could prevent protein synthesis alteration and neurodegeneration that contributed to the beneficial effect of fullerene (Makarova et al. 2012). Further, the protective effects of fullerene on neuroplasticity was found in another Alzheimer's disease rat model infused with $A\beta_{1–42}$ protein in improving the cortical and hippocampal EEG interplay (Vorobyov et al. 2015). Recent works by Troshin and co-workers also confirmed the neuroprotective effects of fullerene derivatives as a potential brain medicine (Hsieh et al. 2017; Kotelnikova et al. 2014), and the anti-amyloid activity of fullerenolates was demonstrated with electron microscopic results (Bobylev et al. 2011) suggesting their potential applications in neurodegenerative diseases. These results implied that in brains with high oxidative stress, fullerene may play a beneficial role due to its excellent anti-oxidative and free radical scavenger properties, along with other potential benefits.

In spite of the enormous studies on fullerene derivatives, un-modified fullerene was still the main component exposed to the human body, and the investigation of un-modified fullerene effect on learning and memory abilities of subjects with different pathological conditions was novel and important. In our study, we monitored the effect of chronic treatment (two weeks) of fullerene particles at a cytotoxic dosage (50 mg/kg) that caused impairment of spatial learning and memory abilities of sham/non-dementia mice along with LTP suppression that agreed with previous literatures (Tsuchiya et al. 1996), probably due to lipid peroxidation and elevated oxidative stress caused by fullerene (Oberdörster 2004; Sayes et al. 2005; Usenko et al. 2008). Interestingly when administering fullerene at the same toxically high dosage for two weeks, the learning and memory abilities and LTP effects of SIVD model mice were not impaired, but tended to be improved as demonstrated in this study. These results imply that even at such a high dosage, cytotoxic to sham mice, fullerene plays a beneficial role on SIVD mice.

Under vascular ischemia, biological properties of the brain may be subjected to alterations, such as disrupted BBB and white matter injury (Ihara and Tomimoto 2011) along with elevated oxidative stress (Friberg et al. 2002; Love 1999; Radak et al. 2013). Dendritic spines are postsynaptic components of most excitatory synapses that serve as the important structural basis of neuroplasticity (Bhatt et al. 2009) and play important roles in the pathological development of neurodegenerative diseases (Herms and Dorostkar 2016). In our study, we observed the suppression of dendritic spine densities in SIVD mice that agreed with previous reports on ischemia (Enright et al. 2007). The dendritic spine density suppression would contribute to learning and memory impairment of SIVD mice observed in our study and agreed with previous literatures (Ihara and Tomimoto 2011). In accordance with the results of MWM and LTP, fullerene played different roles on sham vs. SIVD mice on suppressing the dendritic spine densities of sham mice but tended to be improved with that of SIVD mice, which agreed with our hypothesis.

To further reveal the underlying mechanism of the effect of fullerene on neuroplasticity, we investigate important proteins that tightly regulated or mediated neuroplasticity. Our results demonstrated that the effect of fullerene on neuroplasticity was mainly conducted through a postsynaptic regulation and mediated by BDNF. BDNF was reported to be protective against hypoxia-ischemia (Han et al. 2000; Han and Holtzman 2000) and could rescue spatial memory deficits against ischemia (Almli et al. 2000). In our study, we observed a recovery of BDNF on SIVD mice treated with fullerene, along with improved MWM test outcomes that agreed with these literatures. In this study, though the impact on BDNF contents was confirmed, no obvious alteration on TrkB, the receptor of BDNF on the cellular membrane, was observed. In future studies, other possible signaling pathways that involved BDNF should be tested to further understand the underlying mechanism.

Conclusion

In this study, we have demonstrated distinct effects of fullerene, a widely used carbon material in ecosystem de-contamination and modern medicine on sham vs. SIVD mice. Though fullerene showed a harmful effect on both cognition and underlying neuroplasticity of sham mice, fullerene did improve these abilities/properties of SIVD mice. Our study provided useful insights to treating subjects with different pathological conditions for future application of fullerene in drug development as well as environment de-contamination.

Author Contributions Y. Wu, R. Wang, and Y. Wang equally contributed to this study. Y. Wu and R. Wang conducted most of the experiments and part of data analysis. Y. Wang designed experiments, conducted data analysis, and prepared the manuscript. J. Gao and L. Feng designed and conducted some of the experiments. Z. Yang designed the experiments and prepared the manuscript.

Funding Information This study was financially supported by grants from the National Natural Science Foundation of China (81571804, 81771979 from Z. Yang) and China Postdoctoral Science Foundation (2016M601250 from Y. Wang).

Compliance with Ethical Standards

Conflict of Interest The authors declare that they have no conflicts of interest.

References

Ali SS, Hardt JI, Dugan LL (2008) SOD activity of carboxyfullerenes predicts their neuroprotective efficacy: a structure-activity study. Nanomedicine 4:283–294

Ali SS, Hardt JI, Quick KL, Kimhan JS, Erlanger BF, Huang TT, Epstein CJ, Dugan LL (2004) A biologically effective fullerene (C60) derivative with superoxide dismutase mimetic properties. Free Radic Biol Med 37:1191–1202

Almli CR, Levy TJ, Han BH, Shah AR, Gidday JM, Holtzman DM (2000) BDNF protects against spatial memory deficits following neonatal hypoxia-ischemia. Exp Neurol 166:99–114

An L, Liu S, Yang Z, Zhang T (2012) Cognitive impairment in rats induced by nano-CuO and its possible mechanisms. Toxicol Lett 213:220–227

Bhatt DH, Zhang S, Gan WB (2009) Dendritic spine dynamics. Annu Rev Physiol 71:261–282

Bobylev AG, Kornev AB, Bobyleva LG, Shpagina MD, Fadeeva IS, Fadeev RS, Deryabin DG, Balzarini J, Troshin PA, Podlubnaya ZA (2011) Fullerenolates: metallated polyhydroxylated fullerenes with potent anti-amyloid activity. Org Biomol Chem 9:5714–5719

Chae S-R, Hotze EM, Wiesner MR (2014) Chapter 21 - possible applications of fullerene nanomaterials in water treatment and reuse A2 - street, Anita. In: Sustich R, Duncan J, Savage N (eds) Nanotechnology applications for clean water (second edition). William Andrew Publishing, Oxford, pp 329–338

Cunha C, Brambilla R, Thomas K (2010) A simple role for BDNF in learning and memory? Front Mol Neurosci 3:1–14

Dugan LL, Gabrielsen JK, Yu SP, Lin T-S, Choi DW (1996) Buckminsterfullerenol free radical scavengers reduce excitotoxic and apoptotic death of cultured cortical neurons. Neurobiol Dis 3:129–135

Dugan LL, Lovett EG, Quick KL, Lotharius J, Lin TT, O'Malley KL (2001) Fullerene-based antioxidants and neurodegenerative disorders. Parkinsonism Relat Disord 7:243–246

Dugan LL, Tian LL, Quick KL, Hardt JI, Karimi M, Brown C, Loftin S, Flores H, Moerlein SM, Polich J (2014) Carboxyfullerene neuroprotection postinjury in parkinsonian nonhuman primates. Ann Neurol 76:393–402

Dugan LL, Turetsky DM, Du C, Lobner D, Wheeler M, Almli CR, Luh TY, Choi DW, Lin TS (1997) Carboxyfullerenes as neuroprotective agents. Proc Natl Acad Sci U S A 94:9434–9439

Dumitriu D, Rodriguez A, Morrison J (2011) High-throughput, detailed, cell-specific neuroanatomy of dendritic spines using microinjection and confocal microscopy. Nat Protoc 6:1391–1411

Enright LE, Zhang S, Murphy TH (2007) Fine mapping of the spatial relationship between acute ischemia and dendritic structure indicates selective vulnerability of layer V neuron dendritic tufts within single neurons in vivo. J Cereb Blood Flow Metab Off J Int Soc Cereb Blood Flow Metab 27:1185–1200

Friberg H, Wieloch T, Castilho RF (2002) Mitochondrial oxidative stress after global brain ischemia in rats. Neurosci Lett 334:111–114

Gao J, Zhang X, Yu M, Ren G, Yang Z (2015) Cognitive deficits induced by multi-walled carbon nanotubes via the autophagic pathway. Toxicology 337:21–29

Geckeler KE, Samal S (2001) Rapid assessment of the free radical scavenging property of fullerenes. Fuller Sci Technol 9:17–23

Gordon R, Podolski I, Makarova E, Deev A, Mugantseva E, Khutsyan S, Sengpiel F, Murashev A, Vorobyov V (2017) Intrahippocampal pathways involved in learning/memory mechanisms are affected by intracerebral infusions of amyloid-β25-35 peptide and hydrated fullerene C60 in rats. J Alzheimers Dis Jad 58:1–14

Gottmann K, Mittmann T, Lessmann V (2009) BDNF signaling in the formation, maturation and plasticity of glutamatergic and GABAergic synapses. Exp Brain Res 199:203–234

Han BH, D'Costa A, Back SA, Parsadanian M, Patel S, Shah AR, Gidday JM, Srinivasan A, Deshmukh M, Holtzman DM (2000) BDNF blocks caspase-3 activation in neonatal hypoxia-ischemia. Neurobiol Dis 7:38–53

Han BH, Holtzman DM (2000) BDNF protects the neonatal brain from hypoxic-ischemic injury in vivo via the ERK pathway. J Neurosci 20:5775–5781

Han G, An L, Yang B, Si L, Zhang T (2013) Nicotine-induced impairments of spatial cognition and long-term potentiation in adolescent male rats. Hum Exp Toxicol 33:203–213

Herms J, Dorostkar MM (2016) Dendritic spine pathology in neurodegenerative diseases. Annu Rev Pathol 11:221–250

Hsieh F-Y, Zhilenkov AV, Voronov II, Khakina EA, Mischenko DV, Troshin PA, Hsu S-h (2017) Water-soluble fullerene derivatives as brain medicine: surface chemistry determines if they are neuroprotective and antitumor. ACS Appl Mater Interfaces 9:11482–11492

Hunt CA, Schenker LJ, Kennedy MB (1996) PSD-95 is associated with the postsynaptic density and not with the presynaptic membrane at forebrain synapses. J Neurosci 16:1380–1388

Ihara M, Tomimoto H (2011) Lessons from a mouse model characterizing features of vascular cognitive impairment with white matter changes. J Aging Res 2011:978761

Irie K, Nakamura Y, Ohigashi H, Tokuyama H, Yamago S, Nakamura E (1996) Photocytotoxicity of water-soluble fullerene derivatives. Biosci Biotechnol Biochem 60:1359–1361

Ishii A, Ohkoshi N, Yoshida M, Tamaoka A (2013) P.19.8 the effect of water-soluble fullerene with different number of hydroxyl groups in muscle regeneration process of experimental murine skeletal muscle. Neuromuscul Disord 23:838

Ishii A, Yoshida M, Ohkoshi N, Ueno H, Kokubo K, Tamaoka A (2014) G.P.204: the effect of water-soluble fullerene in muscle regeneration process. Neuromuscul Disord 24:878

Kotelnikova RA, Smolina AV, Grigoryev VV, Faingold II, Mischenko DV, Rybkin AY, Poletayeva DA, Vankin GI, Zamoyskiy VL, Voronov II, Troshin PA, Kotelnikov AI, Bachurin SO (2014) Influence of water-soluble derivatives of [60]fullerene on therapeutically important targets related to neurodegenerative diseases. MedChemComm 5:1664–1668

Kroto HW, Heath JR, O'Brien SC, Curl RF, Smalley RE (1985) C60: Buckminsterfullerene. Nature 318:162–163

Leßmann V, Brigadski T (2009) Mechanisms, locations, and kinetics of synaptic BDNF secretion: an update. Neurosci Res 65:11–22

Love S (1999) Oxidative stress in brain ischemia. Brain Pathol 9:119–131

Lu B (2003) BDNF and activity-dependent synaptic modulation. Learn Mem 10:86–98

Lyon DY, Fortner JD, Sayes CM, Colvin VL, Hughe JB (2010) Bacterial cell association and antimicrobial activity of a C60 water suspension. Environ Toxicol Chem 24:2757–2762

Makarova EG, Gordon RY, Podolski IY (2012) Fullerene C60 prevents neurotoxicity induced by intrahippocampal microinjection of amyloid-beta peptide. J Nanosci Nanotechnol 12:119–126

Murín R, Drgová A, Kaplán P, Dobrota D, Lehotský J (2001) Ischemia/reperfusion-induced oxidative stress causes structural changes of brain membrane proteins and lipids. Gen Physiol Biophys 20:431–438

Narayanan SN, Jetti R, Gorantla VR, Kumar RS, Nayak S, Bhat PG (2014) Appraisal of the effect of brain impregnation duration on neuronal staining and morphology in a modified Golgi–Cox method. J Neurosci Methods 235:193–207

Narita M, Nishiumi H, Sato C, Amano F (2004) Water treatment application of C60-C70 fullerene as visible light sensitizer. Asian Pacific Confederation of Chemical Engineering congress program and abstracts 2004: 623–623

Oberdörster E (2004) Manufactured nanomaterials (fullerenes, C60) induce oxidative stress in the brain of juvenile largemouth bass. Environ Health Perspect 112:1058–1062

Paxinos G, Franklin K (2007) The mouse brain in stereotaxic coordinates. El Sevier Academic Press

Podlubnaya ZA, Podol'Skii IY, Shpagina MD, Marsagishvili LG (2006) Electron microscopic study of the effect of fullerene on the formation of amyloid fibrils by the Aβ 25–35 peptide. Biophysics - Pergamon- C/C of Biofizika 51:701–704

Podolski IY, Podlubnaya ZA, Godukhin OV (2010) Fullerenes C 60 , antiamyloid action, the brain, and cognitive processes. Biophysics 55:71–76

Podolski IY, Podlubnaya ZA, Kosenko EA, Mugantseva EA, Makarova EG, Marsagishvili LG, Shpagina MD, Kaminsky YG, Andrievsky GV, Klochkov VK (2007) Effects of hydrated forms of C60 fullerene on amyloid 1-peptide fibrillization in vitro and performance of the cognitive task. J Nanosci Nanotechnol 7:1479–1485

Prylutskyy YI, Vereshchaka IV, Maznychenko AV, Bulgakova NV, Gonchar OO, Kyzyma OA, Ritter U, Scharff P, Tomiak T, Nozdrenko DM, Mishchenko IV, Kostyukov AI (2017) C60 fullerene as promising therapeutic agent for correcting and preventing skeletal muscle fatigue. J Nanobiotechnol 15:8

Quick KL, Ali SS, Arch R, Xiong C, Wozniak D, Dugan LL (2008) A carboxyfullerene SOD mimetic improves cognition and extends the lifespan of mice. Neurobiol Aging 29:117–128

Radak D, Resanovic I, Isenovic ER (2013) Link between oxidative stress and acute brain ischemia. Angiology 65:667–676

Rodriguez A, Ehlenberger DB, Dickstein DL, Hof PR, Wearne SL (2008) Automated three-dimensional detection and shape classification of dendritic spines from fluorescence microscopy images. PLoS One 3: e1997

Sayes CM, Gobin AM, Ausman KD, Mendez J, West JL, Colvin VL (2005) Nano-C60 cytotoxicity is due to lipid peroxidation. Biomaterials 26:7587–7595

Sayes CM, Marchione AA, Reed KL, Warheit DB (2007) Comparative pulmonary toxicity assessments of C60 water suspensions in rats: few differences in fullerene toxicity in vivo in contrast to in vitro profiles. Nano Lett 7:2399–2406

Squire LR (2004) Memory systems of the brain: a brief history and current perspective. Neurobiol Learn Mem 82:171–177

Tsuchiya T, Oguri I, Yamakoshi YN, Miyata N (1996) Novel harmful effects of [60]fullerene on mouse embryos in vitro and in vivo. FEBS Lett 393:139–145

Usenko CY, Harper SL, Tanguay RL (2007) In vivo evaluation of carbon fullerene toxicity using embryonic zebrafish. Carbon 45:1891–1898

Usenko CY, Harper SL, Tanguay RL (2008) Fullerene C60 exposure elicits an oxidative stress response in embryonic zebrafish. Toxicol Appl Pharmacol 229:44–55

Vorobyov V, Kaptsov V, Gordon R, Makarova E, Podolski I, Sengpiel F (2015) Neuroprotective effects of hydrated fullerene C60: cortical and hippocampal EEG interplay in an amyloid-infused rat model of Alzheimer's disease. J Alzheimers Dis 45:217–233

Yamago S, Tokuyama H, Nakamura E, Kikuchi K, Kananishi S, Sueki K, Nakahara H, Enomoto S, Ambe F (1995) In vivo biological behavior of a water-miscible fullerene: 14C labeling, absorption, distribution, excretion and acute toxicity. Chem Biol 2:385–389

Yamawaki H, Iwai N (2006) Cytotoxicity of water-soluble fullerene in vascular endothelial cells. Am J Phys Cell Phys 290(6):C1495–C1502

Yin G, Xu Z (2002) Synthesis of water-soluble C 60 derivatives and their scavenging free radical activity. SCIENCE CHINA Chem 45:54–59

Yin JJ, Lao F, Fu PP, Wamer WG, Zhao Y, Wang PC, Qiu Y, Sun B, Xing G, Dong J (2009) The scavenging of reactive oxygen species and the potential for cell protection by functionalized fullerene materials. Biomaterials 30:611–621

Yudoh K, Karasawa RF, Masuko K, Fau - Kato T, Kato T (2009a) Water-soluble fullerene (C60) inhibits the development of arthritis in the rat model of arthritis. Int J Nanomedicine 4:217–225

Yudoh K, Karasawa R, Masuko K, Kato T (2009b) Water-soluble fullerene (C60) inhibits the osteoclast differentiation and bone destruction in arthritis. Int J Nanomedicine 4:233–239

Zhou Z (2013) Liposome formulation of fullerene-based molecular diagnostic and therapeutic agents. Pharmaceutics 5(4):525–541